

Four-State Switching Characteristics of  
a Gated Molecular Basket

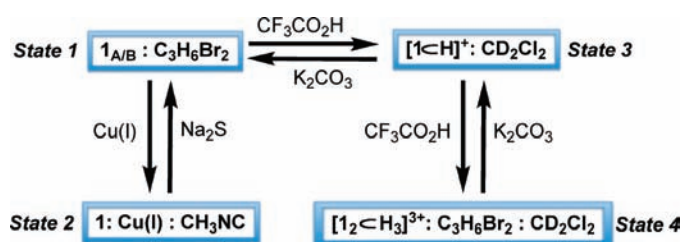
Stephen Rieth, Bao-Yu Wang, Xiaoguang Bao, and Jovica D. Badjić\*

Department of Chemistry, The Ohio State University, 100 West 18th Avenue,  
Columbus, Ohio 43210

badjic@chemistry.ohio-state.edu

Received February 7, 2009

## ABSTRACT



The development of working molecular devices relies on the ability to extrinsically modulate function via structure. We have found that gated molecular basket **1** can be reversibly interconverted among four unique structural states (see above). Controlling the relative population of these states, the recognition characteristics of the basket can be finely tuned.

The action of biological molecules is often regulated via conformational changes that enable the reversible switching of their tertiary/quaternary structure.<sup>1,2</sup> Likewise, tunable abiotic hosts have been made to alter affinity/selectivity (function) when prompted with an external stimulus.<sup>3</sup> Diederich and co-workers have thus introduced quinoxaline-bridged roseorcing[4]arene cavitands as two-state molecular switches for regulating the inner-phase occupancy of these hosts.<sup>3c</sup> Despite the advancements in the field, attaining control over the conformational dynamics, and thus functional behavior of hosts remains a challenge.<sup>4</sup> The understanding of structure/function relationships is expected to

assist efforts toward obtaining more effective catalysts,<sup>5a</sup> energy conversion devices<sup>5b</sup> and trafficking modules.<sup>5c</sup>

The present study, accordingly, is focused on examining the capacity of a new host, molecular basket **1**, for altering its structure, and thereby function, when prompted with an external stimulus (Figure 1).<sup>6</sup> The basket has been shown to respond to its environment by giving rise to four different structural states. Each state is characterized by unique encapsulation behavior, presenting this dynamic host as an intricate four-state molecular switch.<sup>7</sup>

(1) (a) Cui, Q.; Karplus, M. *Protein Sci.* **2008**, *17*, 1295–1307. (b) Goodey, N. M.; Benkovic, S. J. *Nat. Chem. Biol.* **2008**, *4*, 474–482.

(2) (a) Dougherty, D. A. *Chem. Rev.* **2008**, *108*, 1642–1653. (b) Hanek, A. P.; Lester, H. A.; Dougherty, D. A. *J. Am. Chem. Soc.* **2008**, *130*, 13216–13218.

(3) (a) Shinkai, S.; Ogawa, T.; Nakaji, T.; Kusano, Y.; Nanabe, O. *Tetrahedron Lett.* **1979**, *19*, 4569–4572. (b) Xu, H.; Stamp, S. P.; Rudkevich, D. M. *Org. Lett.* **2003**, *5*, 4583–4586. (c) Gottschalk, T.; Jaun, B.; Diederich, F. *Angew. Chem., Int. Ed.* **2007**, *46*, 260–264. (d) Lemieux, V.; Spantulescu, M. D.; Baldrige, K. K.; Branda, N. R. *Angew. Chem., Int. Ed.* **2008**, *120*, 5034–5037.

(4) (a) Davis, A. V.; Yeh, R. M.; Raymond, K. N. *Proc. Nat. Acad. Sci. U.S.A.* **2002**, *99*, 4793–4796. (b) Myong, S.; Stevens, B. C.; Ha, T. *Structure* **2006**, *14*, 633–643.

(5) (a) *Supramolecular Catalysis*; van Leeuwen, P. V. N. M., Ed.; Wiley-VCH: Weinheim, 2008. (b) Balzani, V.; Credi, A.; Venturi, M. *Molecular Devices and Machines*; Wiley-VCH: Weinheim, 2003. (c) Sakai, N.; Mareda, J.; Matile, S. *Mol. Biosyst.* **2007**, *3*, 658–666.

(6) (a) Maslak, V.; Yan, Z.; Xia, S.; Gallucci, J.; Hadad, C. M.; Badjić, J. D. *J. Am. Chem. Soc.* **2006**, *128*, 5887–5894. (b) Rieth, S.; Yan, Z.; Xia, S.; Gardlik, M.; Chow, A.; Fraenkel, G.; Hadad, C. M.; Badjić, J. D. *J. Org. Chem.* **2008**, *73*, 5100–5109. (c) Wang, B.-Y.; Rieth, S.; Badjić, J. D. *J. Am. Chem. Soc.* **2009**, *131*, 7250–7252.

(7) (a) *Molecular Switches*; Feringa, B. L., Ed.; Wiley-VCH: Weinheim, 2001. (b) Moonen, N. N. P.; Flood, A. H.; Fernandez, J. M.; Stoddart, J. F. *Top. Curr. Chem.* **2005**, *262*, 99–132. (c) Cheng, K.-W.; Lai, C.-C.; Chiang, P.-T.; Chiu, S.-H. *Chem. Commun.* **2006**, 2854–2856. (d) de Silva, A. P. *Nature* **2008**, *454*, 417–418.

(8) (a) Wang, B.-Y.; Bao, X.; Yan, Z.; Maslak, V.; Hadad, C. M.; Badjić, J. D. *J. Am. Chem. Soc.* **2008**, *130*, 15127–15133. (b) Wang, B.-Y.; Bao, X.; Stojanovic, S.; Hadad, C. M.; Badjić, J. D. *Org. Lett.* **2008**, *10*, 5361–5364.

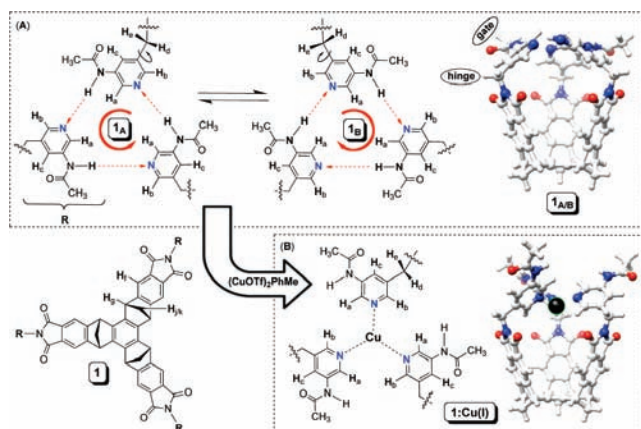


**Figure 1.** Chemical structures of hydrogen bonded (**1**<sub>A/B</sub>, A) and Cu(I) folded (**1**:Cu(I), B) basket **1**. Side views of energy minimized (DFT, B3LYP) structures of **1**<sub>A/B</sub> (top) and **1**:Cu(I) (bottom).

**Hydrogen-Bonded Basket 1<sub>A/B</sub>.** Molecular basket **1** has been designed to contain three pyridine-based gates, linked via intramolecular hydrogen bonding (HB) from *meta* amido groups, to occlude space and thus form a dynamic and gated environment (Figure 1A).<sup>8</sup> The downfield <sup>1</sup>H NMR chemical shift ( $\delta = 10.8$  ppm, Figure 2A) of the N–H resonances

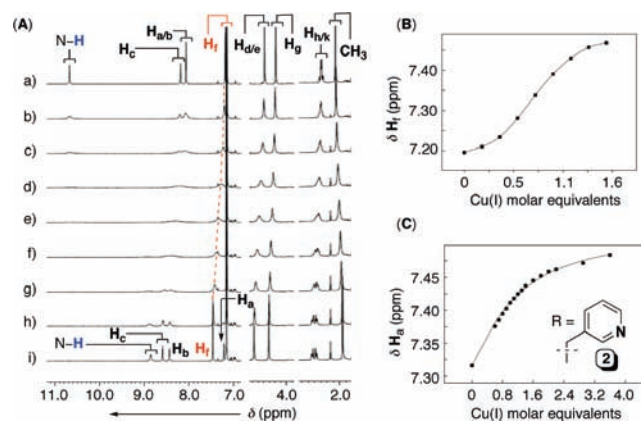


**Figure 2.** (A) Selected regions of <sup>1</sup>H NMR spectra (400 MHz, 298 K) of **1** (1.9 mM, CD<sub>2</sub>Cl<sub>2</sub>/C<sub>6</sub>D<sub>6</sub> = 2:1) recorded after addition of: (a) 6, (b) 12, (c) 18, (d) 24, (e) 30, (f) 36, (g) 42, (h) 48, and (i) 54 μL of 17.4 mM solution of (CuOTf)<sub>2</sub>PhMe. (B) <sup>1</sup>H NMR chemical shifts of the **H<sub>f</sub>** resonance in **1** (1.9 mM) as a function of the titrated (CuOTf)<sub>2</sub>PhMe (17.4 mM). (C) <sup>1</sup>H NMR chemical shifts of the **H<sub>a</sub>** resonance in **2** (2.5 mM) as a function of the titrated (CuOTf)<sub>2</sub>PhMe (32.5 mM).

indicates the intramolecular HB contacts.<sup>8a</sup> The “hinge” **H<sub>d/e</sub>** spins appeared as a singlet at high temperatures and as an AB quartet at low temperatures, thus demonstrating the interconversion of two C<sub>3</sub> symmetric enantiomers, **1<sub>A</sub>** and **1<sub>B</sub>**, each containing hydrogen bonds displayed in the clockwise or the counter-clockwise orientation (Figures S5/6, Supporting Information).<sup>9</sup> In essence, the **1<sub>A/B</sub>** intercon-

version necessitates that each of the gates revolve 180° about the “vertical” axis. The activation energy ( $\Delta G^{\ddagger}_{298}$ ) for this internal motion was found to be on the order of 10.8 kcal/mol, from NMR line-shape analysis.<sup>9</sup>

**Cu(I) Folded Basket 1. Cu(I).** Upon an incremental addition of a standard solution of (CuOTf)<sub>2</sub>PhMe to **1<sub>A/B</sub>**, the basket’s <sup>1</sup>H NMR spectrum changed: (a) the N–H resonance shifted upfield ( $\Delta\delta = 2.0$  ppm) and (b) the aromatic **H<sub>b/c/f</sub>** resonances moved downfield (Figure 2A). Evidently, the addition of Cu(I) disrupted the intramolecular N–H...N contacts in **1<sub>A/B</sub>** and promoted the formation of another C<sub>3</sub> symmetric assembly. Indeed, the results of <sup>1</sup>H NMR DOSY, COSY, NOESY spectroscopic and MALDI spectrometric measurements (Figures S1–S4, Supporting Information)<sup>9</sup> suggested the existence of **1**:Cu(I) (Figure 1B). When the chemical shift for the **H<sub>f</sub>** resonance was plotted against the molar equivalents of Cu(I) added to **1<sub>A/B</sub>**, a sigmoidal dependence was evident (Figure 2B). Perhaps, the formation of the **1**:Cu(I) complex occurred stepwise with some degree of cooperativity.<sup>12</sup> Molecular basket **2**, with freely rotating pyridine gates (i.e., without amido groups), was previously shown to bind Cu(I), thereby yielding **2**:Cu(I) complex (Figure 2C).<sup>6b</sup> Interestingly, the assembling of **2**:Cu(I) (Figure 2B) required a greater quantity of copper than the formation of **1**:Cu(I) (Figure 2C). The finding that it is “easier” to coordinate **1** than **2** to Cu(I) is intriguing; the electronic/steric substituent effects of the meta amides, evidently, played a role in the binding thermodynamics.

**The First Mode of Switching.** Basket **1<sub>A/B</sub>** trapped 2,2-dibromopropane in the presence of methyl isocyanide (Figure 3).<sup>10</sup> The upfield <sup>1</sup>H NMR singlet at  $\delta \sim -0.7$  ppm,

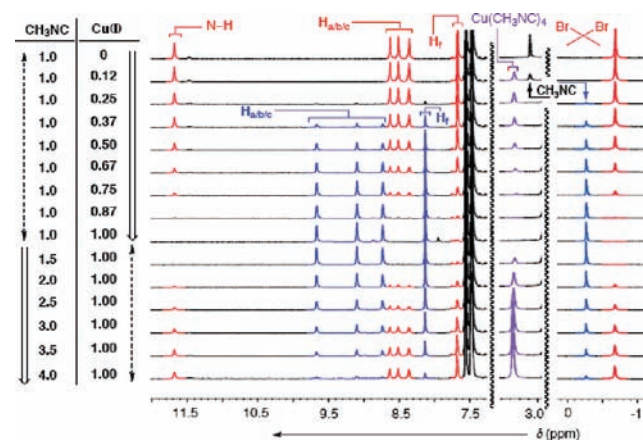


**Figure 3.** Selected regions of <sup>1</sup>H NMR spectra (400 MHz, 243 K) of a solution of basket **1** (1.22 mM, CD<sub>2</sub>Cl<sub>2</sub>/C<sub>6</sub>D<sub>5</sub>CD<sub>3</sub> = 2:1) containing CH<sub>3</sub>CBr<sub>2</sub>CH<sub>3</sub> (19.5 mM) and CH<sub>3</sub>NC (1.22 mM), and recorded after an addition of 13.0 mM (CuOTf)<sub>2</sub>PhMe and 26.0 mM CH<sub>3</sub>NC. Molar equivalents of Cu(I) and CH<sub>3</sub>NC are shown on the left.

corresponding to C<sub>3</sub>H<sub>6</sub>Br<sub>2</sub> inside of **1**, corroborated such an occurrence. Upon addition of Cu(I) to **1<sub>A/B</sub>**,<sup>11</sup> however, the

basket transformed into **1**:Cu(I) entrapping  $\text{CH}_3\text{NC}$  inside its cavity. The disappearance of the resonance at  $-0.7$  ppm and the appearance of another singlet at  $-0.3$  ppm ( $\text{CH}_3\text{NC}$ ) is in accord with that scenario (Figure 3). Interestingly, during the titration, the emergence of  $\text{Cu}(\text{CH}_3\text{NC})_4^+$  ( $\delta = 3.3$  ppm, Figure 3) was observed to precede the formation of **1**:Cu(I): $\text{CH}_3\text{NC}$ . An excess of  $\text{CH}_3\text{NC}$ , however, led to the reappearance of **1**<sub>A/B</sub> (Figure 3). The removal of Cu(I) from **1**:Cu(I): $\text{CH}_3\text{NC}$ , along with the re-encapsulation of  $\text{C}_3\text{H}_6\text{Br}_2$ , was also accomplished with the addition of  $\text{Na}_2\text{S}$  (Figure S7, Supporting Information).<sup>9</sup> Evidently, the basket can be reversibly switched between two structural states with comparable interior volumes<sup>8</sup> of  $\sim 221 \text{ \AA}^3$  and each expressing a unique functional behavior of encapsulation: **1**:Cu(I) showed no affinity for trapping 2,2-dibromopropane (Figure S8, Supporting Information),<sup>9</sup> while **1**<sub>A/B</sub> was not amenable toward encapsulating  $\text{CH}_3\text{NC}$  (Figure S9, Supporting Information). Stoichiometrically balanced equations for the guest-mediated interconversion of Cu(I) folded and hydrogen bonded baskets are shown in Figure 4.

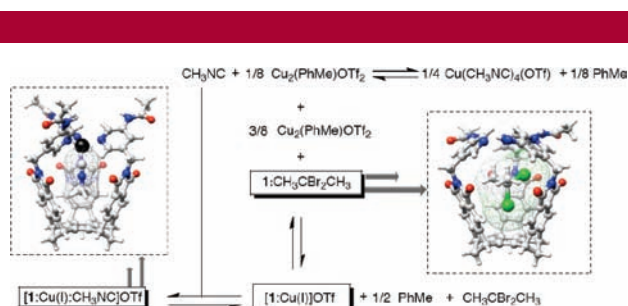


**Figure 4.** Stoichiometrically balanced equations for the conversion of **1**<sub>A/B</sub>:  $\text{CH}_3\text{CBr}_2\text{CH}_3$  into **1**:Cu(I):  $\text{CH}_3\text{NC}$ . Side views of energy minimized (DFT, B3LYP) structures of **1**<sub>A/B</sub>: $\text{CH}_3\text{CBr}_2\text{CH}_3$  (right) and **1**:Cu(I): $\text{CH}_3\text{NC}$  (left).<sup>9</sup>

Presumably, the internal basket's dynamics (in addition to other factors) played an important role for expressing the guest selectivity via the preorganization.<sup>13</sup> The **1**<sub>A/B</sub> interconversion (Figure 1) necessitates the cleavage of  $\text{N}-\text{H}\cdots\text{N}$  hydrogen bond(s) and is energetically demanding (expt  $\Delta G^\ddagger_{298} = 10.8$  kcal/mol, Figure S6, Supporting Information).<sup>9</sup> The analogous conformational change in **1**:Cu(I): $\text{CH}_3\text{NC}$ , however, is more facile and can occur without rupturing the Cu–N coordinative bonds. This dynamic process was not observed experimentally, but computed (DFT, B3LYP) to require a small activation energy ( $\Delta G^\ddagger = 3.9$  kcal/mol, Figure S21, Supporting Information).<sup>9</sup>

**The Second Mode of Switching.** The basket's stimuli-responsive characteristics were further examined under acidic

conditions. The nitrogen atoms, at the pyridine gates in **1**<sub>A/B</sub>, were expected to abstract hydrogen(s) from strong proton donors thereby obstructing the internal hydrogen bonding at the rim of the basket and the encapsulation. An incremental addition of  $\text{CF}_3\text{CO}_2\text{H}$  (TFA) to a solution of **1**<sub>A/B</sub>, containing 2,2-dibromopropane, prompted considerable  $^1\text{H}$  NMR spectroscopic changes (Figure 5). The addition of one molar

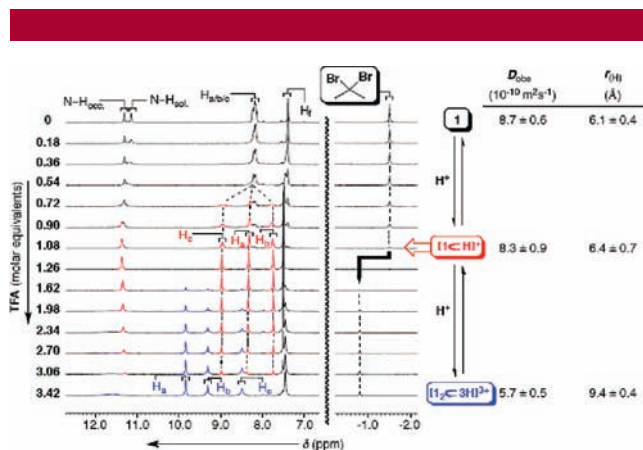


**Figure 5.** Series of  $^1\text{H}$  NMR spectra (400 MHz, 243 K) of a solution of **1** (1.3 mM,  $\text{CD}_2\text{Cl}_2$ ) containing  $\text{CH}_3\text{CBr}_2\text{CH}_3$  (2.2 mM) and recorded after addition of 65.0 mM standard solution of TFA. Diffusion coefficients ( $D_{\text{obs}}$ ) and the corresponding hydrodynamic radii ( $r_{\text{H}}$ ) were obtained from  $^1\text{H}$  NMR DOSY measurements at  $300 \pm 1 \text{ K}$ .<sup>9,14</sup>

equivalent of TFA led to the formation of **[1C<sup>+</sup>H]**<sup>+</sup>; note the occurrence of red-colored signals in Figure 5.  $^1\text{H}$  NMR DOSY, COSY and NOESY spectroscopic measurements suggest the existence of **[1C<sup>+</sup>H]**<sup>+</sup> (Figures S10/11 and S19, Supporting Information).<sup>9</sup> The single protonation, interestingly, initiated the expulsion of 2,2-dibromopropane (Figure 5). At first, the entrapment of trifluoroacetate anion was suspected for contributing to the guest's dismissal. However, the  $\text{CF}_3$  fluorine resonance ( $^{19}\text{F}$  NMR) remained unaffected during the titration, indicating the absence of the TFA encapsulation (Figure S13, Supporting Information).<sup>9</sup> In fact, the shape complementary  $\text{CH}_3\text{SO}_3^-$  anion (from  $\text{CH}_3\text{SO}_3\text{H}$ ) was also shown to reside outside of **[1C<sup>+</sup>H]**<sup>+</sup> (Figure S14, Supporting Information).<sup>9</sup> A molecule of solvent ( $\text{CD}_2\text{Cl}_2$ ) must, therefore, be occupying the singly protonated basket.

Variable temperature  $^1\text{H}$  NMR spectra of **[1C<sup>+</sup>H]**<sup>+</sup> exhibited a set of resonances corresponding to a  $\text{C}_3$  symmetric compound (210–298 K, Figure S12).<sup>9</sup> In particular, a sharp singlet for the hinge  $\text{H}_{\text{d/e}}$  protons and a downfield shifted  $\text{N}-\text{H}$  resonance ( $\delta = 11.2$  ppm) were prominent: the protonated basket comprises a set of rapidly revolving gates interacting via hydrogen bonds; alternatively, more elaborate  $^1\text{H}$  NMR spectra, corresponding to less symmetric structure(s), would be expected.

A Monte Carlo conformational study of **[1C<sup>+</sup>H]**<sup>+</sup> (MMFF force field) provided an insight into the host's dynamics.<sup>9</sup> Three hydrogen bonded and  $\text{C}_s$  symmetric conformers, with

(9) See Supporting Information for more details.

(10) Hydrogen-bonded baskets are known to encapsulate halogenated alkanes (see ref 8b) while Cu-folded baskets entrap  $\text{CH}_3\text{CN}$  (see ref 6b).

(11) In the presence of  $\text{CH}_3\text{NC}$ , the affinity of **1** toward Cu(I) increased so that only one equivalent of Cu(I) was required for the formation of **1**:Cu(I).

(12) (a) Ercolani, G. *J. Am. Chem. Soc.* **2003**, *125*, 16097–16103. (b) Riddle, J. A.; Jiang, X.; Lee, D. *Analyst* **2008**, *133*, 417–422.

(13) Cram, D. J. *Angew. Chem., Int. Ed.* **1986**, *25*, 1039–1057.



a comparable thermodynamic stability of  $E_{\text{steric}} = 0\text{--}3$  kcal/mol, were found.<sup>9</sup> Accordingly, the experimental  $^1\text{H}$  NMR results could be interpreted by a rapid gate-flipping motion assisted with proton shuttling that averaged the hydrogen spins to give a spectrum corresponding to a  $C_3$  symmetric structure. The enhanced dynamics at the rim of  $[\mathbf{1}\text{C}\text{H}]^+$  contributed to the development of a poorly preorganized inner space<sup>13</sup> and, evidently, altered the basket's capacity for acting as a host.

**The Third Mode of Switching.** Further protonation of  $[\mathbf{1}\text{C}\text{H}]^+$  caused the appearance of a new set of  $^1\text{H}$  NMR signals, representing another  $C_3$  symmetric assembly on average, as shown in blue in Figure 5. Notably, the addition of TFA restored the capacity for entrapping 2,2-dibromopropane, whose  $^1\text{H}$  NMR signal shifted further downfield ( $\delta = -0.8$  ppm, Figure 5). Evidently, 2,2-dibromopropane experienced less diamagnetic shielding inside the newly formed host. The trend in the hydrodynamic radii (Figure 5 and Figures S18–S20, Supporting Information),<sup>9</sup> pointed to the basket's aggregation, and possibly assembling into a more sizable dimer. Indeed, when 2,2-dibromopropane was used in excess (to saturate the host), the encapsulation was complete and the integrated basket:guest signal ratio was 2:1 (Figure 6B)! Moreover, the  $C_3$  symmetric nature of  $[\mathbf{1}_2\text{C}\text{H}_3]^{3+}$  concurred with the recorded  $^1\text{H}$  NMR spectrum: two equally strong signals, for each of the  $\text{H}_b/\text{H}_c/\text{H}_f$  protons, correspond to the nuclei residing in the northern and the southern portion of the dimer (Figure 6A). A close proximity of the  $\text{H}_b$  and  $\text{H}_c$  protons was also manifested by the NOE cross signal (Figure S16, Supporting Information).<sup>9</sup> The inner volume of  $[\mathbf{1}_2\text{C}\text{H}_3]^{3+}$ , with the gates pointing to the bulk solvent, was estimated to be  $307 \text{ \AA}^3$ . Guests such as 2,2-dibromopropane ( $105 \text{ \AA}^3$ ) and dichloromethane ( $83 \text{ \AA}^3$ ) occupy  $\sim 61\%$  of the inner space of  $[\mathbf{1}_2\text{C}\text{H}_3]^{3+}$ , accounting for the experimentally observed encapsulation.<sup>15</sup> Ultimately, the addition of  $\text{K}_2\text{CO}_3$  to  $[\mathbf{1}_2\text{C}\text{H}_3]^{3+}$  led to the formation of  $\mathbf{1}_{\text{A/B}}$ , with the transient appearance of  $[\mathbf{1}\text{C}\text{H}]^+$  (Figure S17, Supporting Information).<sup>9</sup> The guest-exchange capacity of the basket can thus be reversibly controlled at yet another level using an acid/base stimulus.

The design and preparation of switchable systems with stimuli-responsive behavior gives access to a variety of versatile materials.<sup>16</sup> The results of our study contribute to such efforts, and demonstrate the adaptive nature of a new family of dynamic and gated hosts. Furthermore, the implementation of function into artificial structures demands

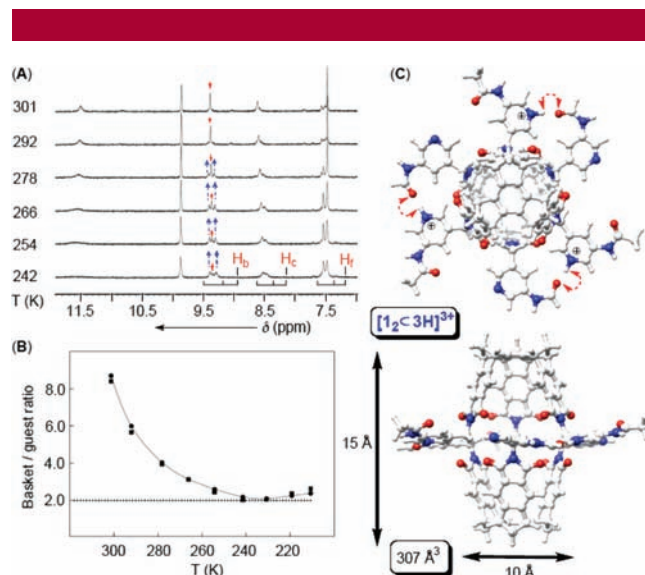


**Figure 6.** (A) Variable temperature  $^1\text{H}$  NMR spectra (500 MHz) of a  $\text{CD}_2\text{Cl}_2$  solution of  $\mathbf{1}$  (0.7 mM) containing 34.0 mM  $\text{CH}_3\text{CBr}_2\text{CH}_3$  and 2.7 mM TFA. (B) Integration proportion ( $^1\text{H}$  NMR) of  $\text{H}_b$  or  $\text{H}_c$  resonances in  $\mathbf{1}$  and the proton nuclei in the encapsulated  $\text{CH}_3\text{CBr}_2\text{CH}_3$  were used to obtain basket/guest ratio as a function of temperature. (C) Top and side views of energy minimized (MMFF) structure of  $[\mathbf{1}_2\text{C}\text{H}_3]^{3+}$ .

a tunable element of design making the described four-state mode of action here a useful paradigm.

**Acknowledgment.** This work was financially supported with funds obtained from the National Science Foundation under CHE-0716355. Generous computational resources were provided by the Ohio Supercomputer Center.

**Supporting Information Available:** Detailed description of experimental methods. This material is available free of charge via the Internet at <http://pubs.acs.org>.

OL9009392

(14) Zuccaccia, D.; Pirondini, L.; Pinalli, R.; Dalcanele, E.; Macchioni, A. *J. Am. Chem. Soc.* **2005**, *127*, 7025–7032.

(15) Mecozzi, S.; Rebek, J., Jr. *Chem. Eur. J.* **1998**, *4*, 1016–1022.

(16) See, for example: (a) Amrhein, P.; Shivanyuk, A.; Johnson, D. W.; Rebek, J., Jr. *J. Am. Chem. Soc.* **2002**, *124*, 10349–10358. (b) Kerckhoffs, J. M. C. A.; van Leeuwen, F. W. B.; Spek, A. L.; Kooijman, H.; Crego-Calama, M.; Reinhoudt, D. N. *Angew. Chem., Int. Ed.* **2003**, *42*, 5717–5722. (c) Badji, J. D.; Balzani, V.; Credi, A.; Silvi, S.; Stoddart, J. F. *Science* **2004**, *303*, 1845–1849. (d) Abe, H.; Masuda, N.; Waki, M.; Inouye, M. *J. Am. Chem. Soc.* **2005**, *127*, 16189–16196. (e) Browne, W. R.; Feringa, B. L. *Nat. Nanotechnol.* **2006**, *1*, 25–35. (f) Chakrabarti, K.; Mukhopadhyay, P.; Lin, S.; Isaacs, L. *Org. Lett.* **2007**, *9*, 2349–2352.